Implementation of an offset-dipole magnetic field in a geometric pulsar emission code

Monica Breed
NWU (Potchefstroom Campus)

Supervisor: Dr. C. Venter
Collaborators: A. K. Harding & T. J. Johnson

Introduction

- The first neutron star (NS) was discovered in 1967 by Jocelyn Bell (Hewish et al. 1968).

- Pulsars: compact, highly magnetized NSs, rotating at tremendous rates.

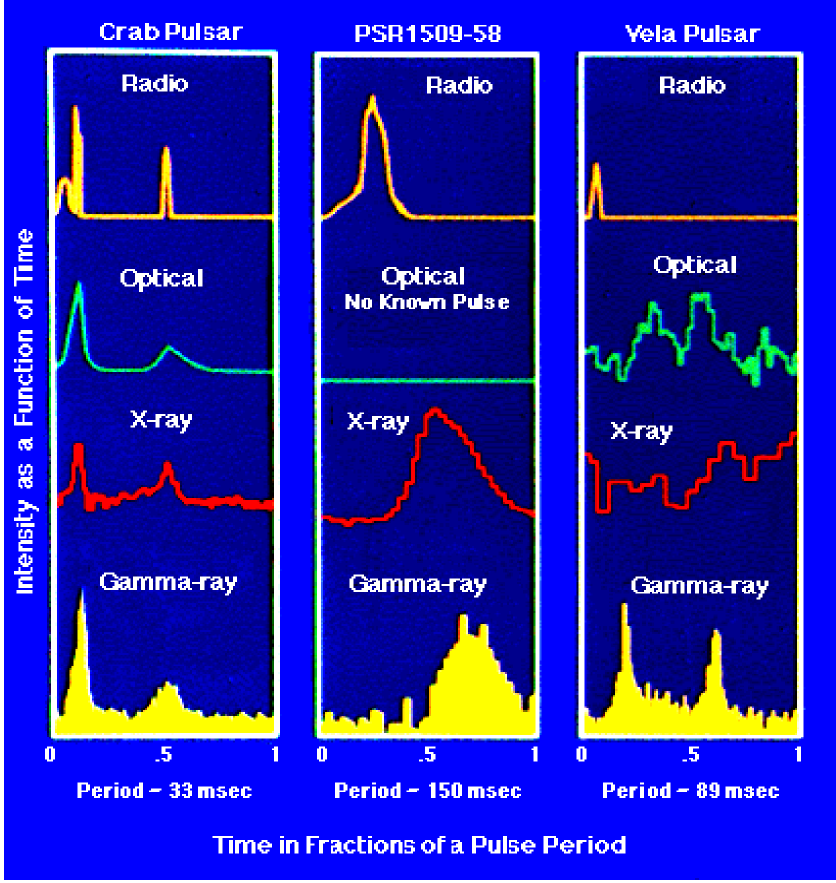

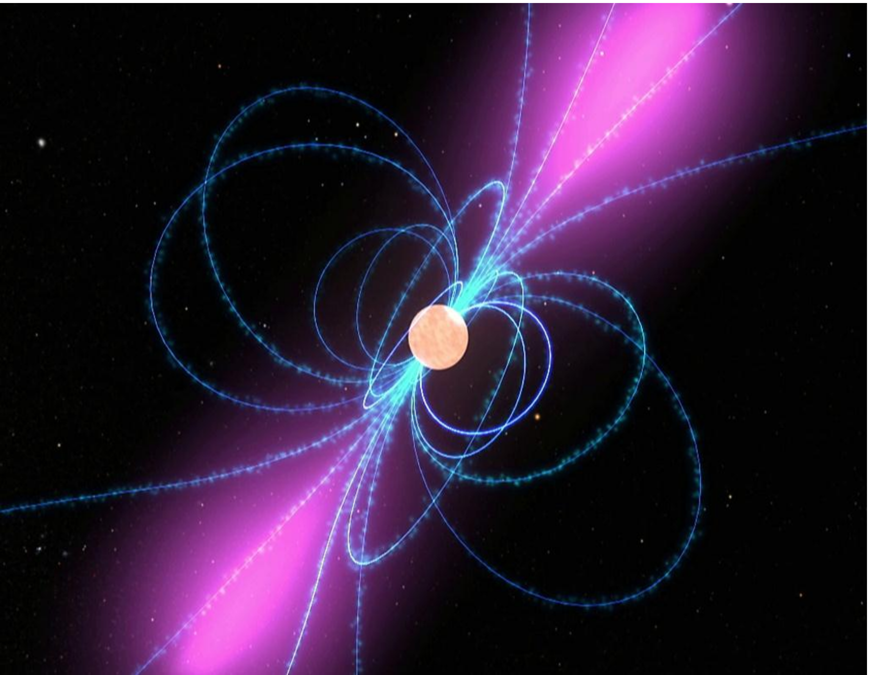

- Emits radiation across the electromagnetic spectrum.

- Focus on γ-ray pulsars (Vela); dominant emission mechanism curvature radiation (CR).

Geometric γ-ray pulsar models

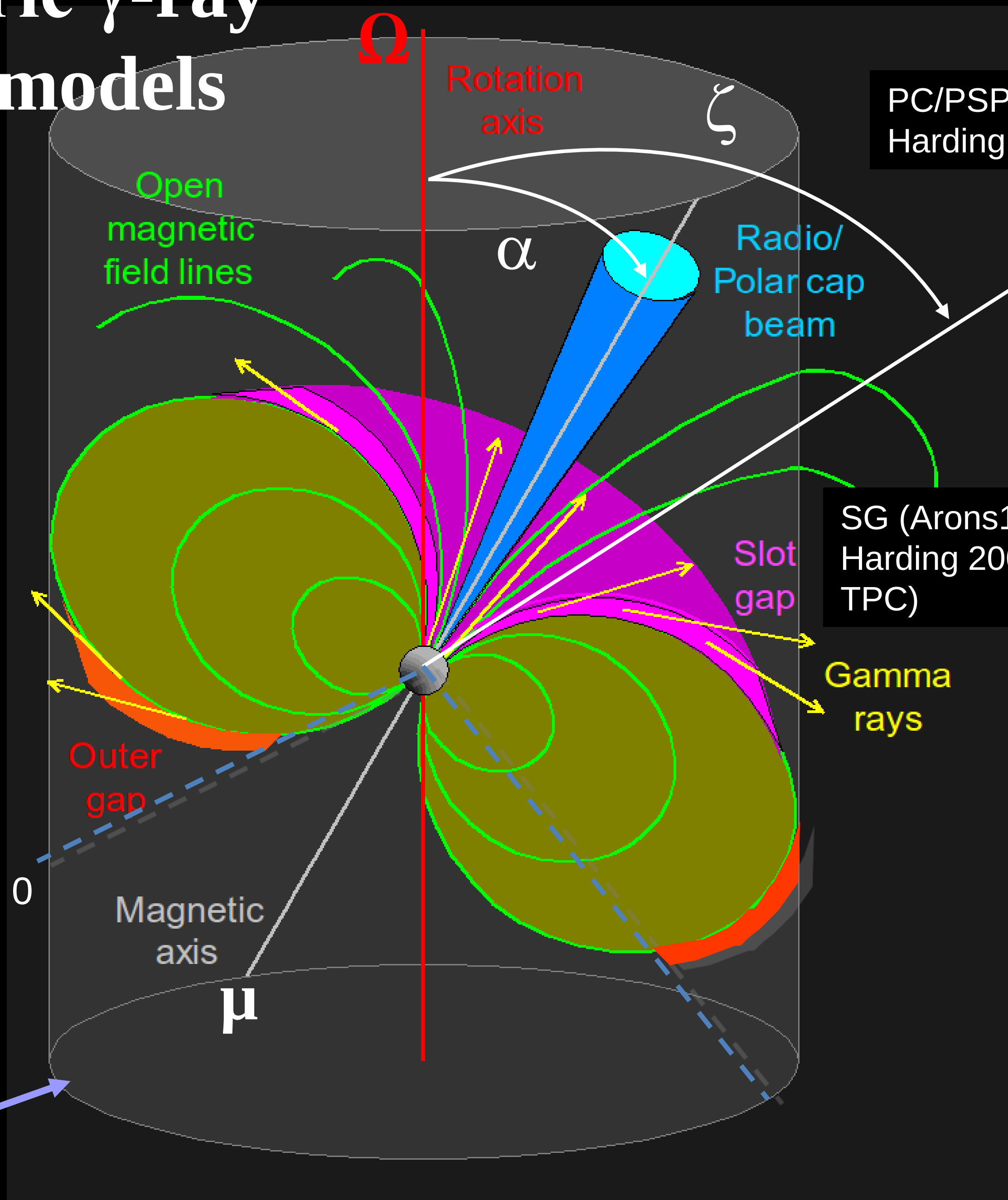

PC/PSPC (Daugherty & Harding 1996; HUM2005)

SG (Arons1983; Muslimov & Harding 2003/4; see Dyks2003 for TPC)

OG
(Cheng et al 1986;
Romani 1996)

Light cylinder

Magnetic fields

Offset-dipole *B*-field

(Harding&Muslimov2011)

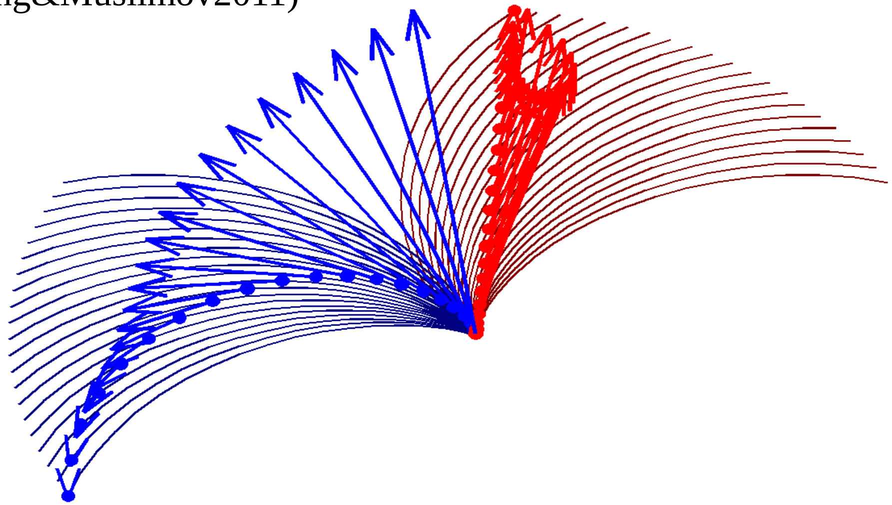

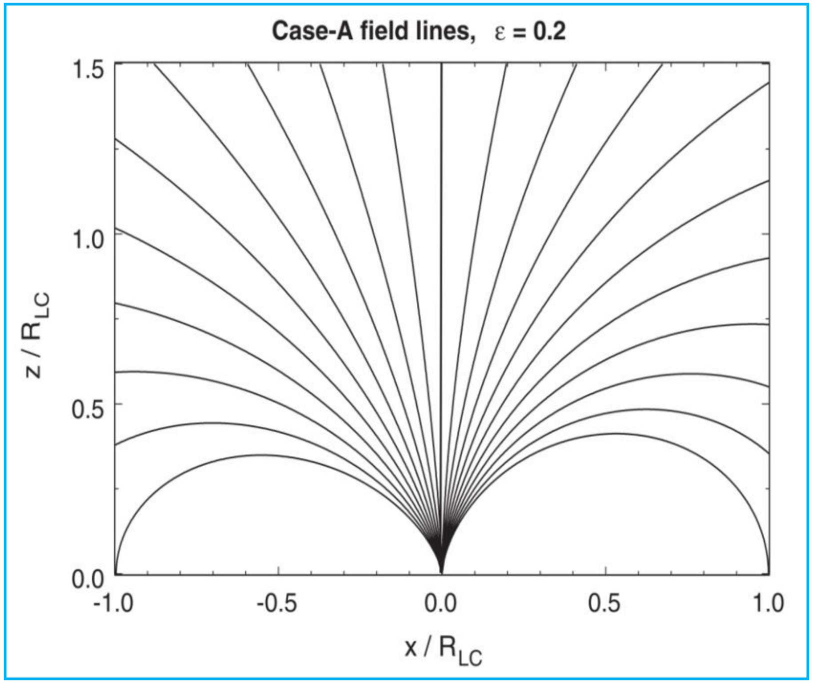

- E.g. due to retardation and asymmetric currents.
- In spherical coordinates, in the $(\hat{\mathbf{z}}' \parallel \boldsymbol{\mu})$ frame (Symmetric case):

$$\mathbf{B}'(r',\theta',\phi') = \frac{\mu}{r'^3}\left[\cos\theta'\hat{\mathbf{r}}' + \frac{1}{2}(1+a)\sin\theta'\hat{\boldsymbol{\theta}}' - \epsilon\sin\theta'\cos\theta'\sin(\phi'-\phi_0)\hat{\boldsymbol{\phi}}'\right]$$

- Offset characterized by parameter ϵ :

$$a = \epsilon\cos(\phi' - \phi_0)$$

- A special case of the static-dipole *B*-field by setting $\epsilon = 0$.

Problem statement

- We studied the effect of implementing an offset-dipole *B*-field on γ-ray LCs.

- Using a TPC emission geometry.

- Solve the particle equation of motion using the offset-dipole SG *E*-field.

- As an application, we compared our model LCs with *Fermi* LAT data for the bright Vela pulsar.

Implementation

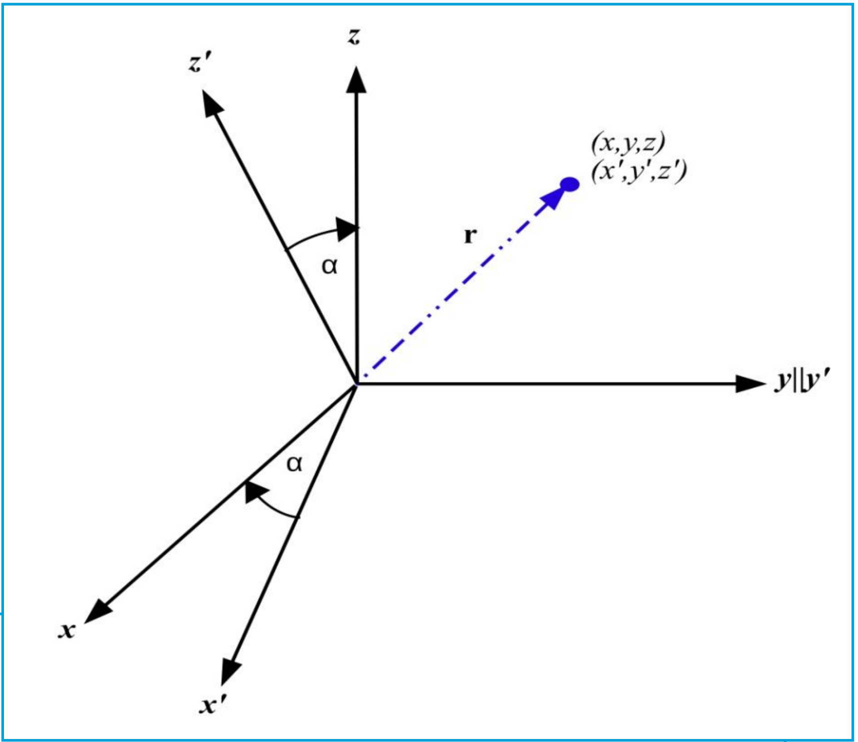

- First transform the *B*-field from spherical to Cartesian coordinate system in $(\hat{\mathbf{z}}' \parallel \boldsymbol{\mu})$ frame:

Transformation:

$$\mathbf{B}'(r',\theta',\phi') = B'_r(r',\theta',\phi')\hat{\mathbf{r}}' + B'_\theta(r',\theta',\phi')\hat{\boldsymbol{\theta}}' + B'_\phi(r',\theta',\phi')\hat{\boldsymbol{\phi}}'$$

$$\mathbf{B}'(x',y',z') = B'_x(x',y',z')\hat{\mathbf{x}}' + B'_y(x',y',z')\hat{\mathbf{y}}' + B'_z(x',y',z')\hat{\mathbf{z}}'$$

- Rotate the Cartesian coordinate system from the $(\hat{\mathbf{z}}' \parallel \boldsymbol{\mu})$ to the $(\hat{\mathbf{z}} \parallel \boldsymbol{\Omega})$ frame through an angle $-\alpha$:

Rotation: $\mathbf{B}(x,y,z) = B_x(x,y,z)\hat{\mathbf{x}} + B_y(x,y,z)\hat{\mathbf{y}} + B_z(x,y,z)\hat{\mathbf{z}}$

Finding the PC rim

$$\Delta r_{\rm PC} \simeq R_{\rm ns}\theta_0\left[1-\theta_0^{\epsilon}\right]$$

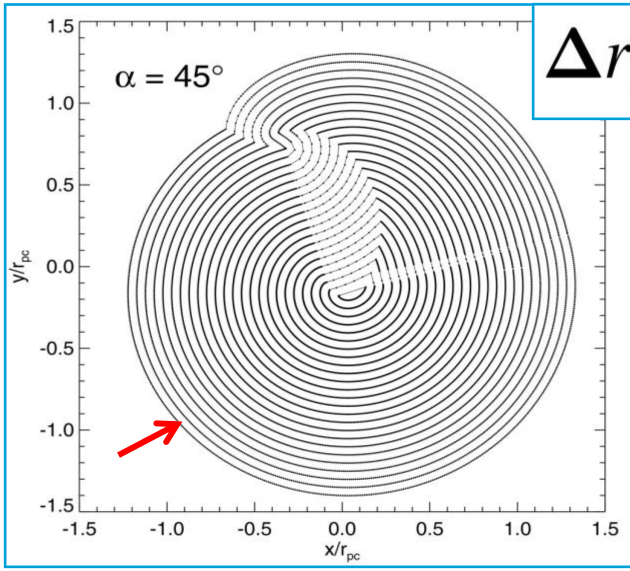

- Expanding parameter space.

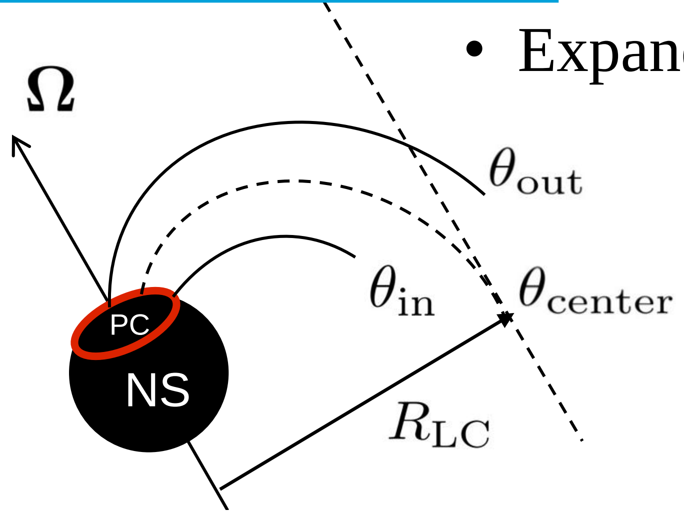

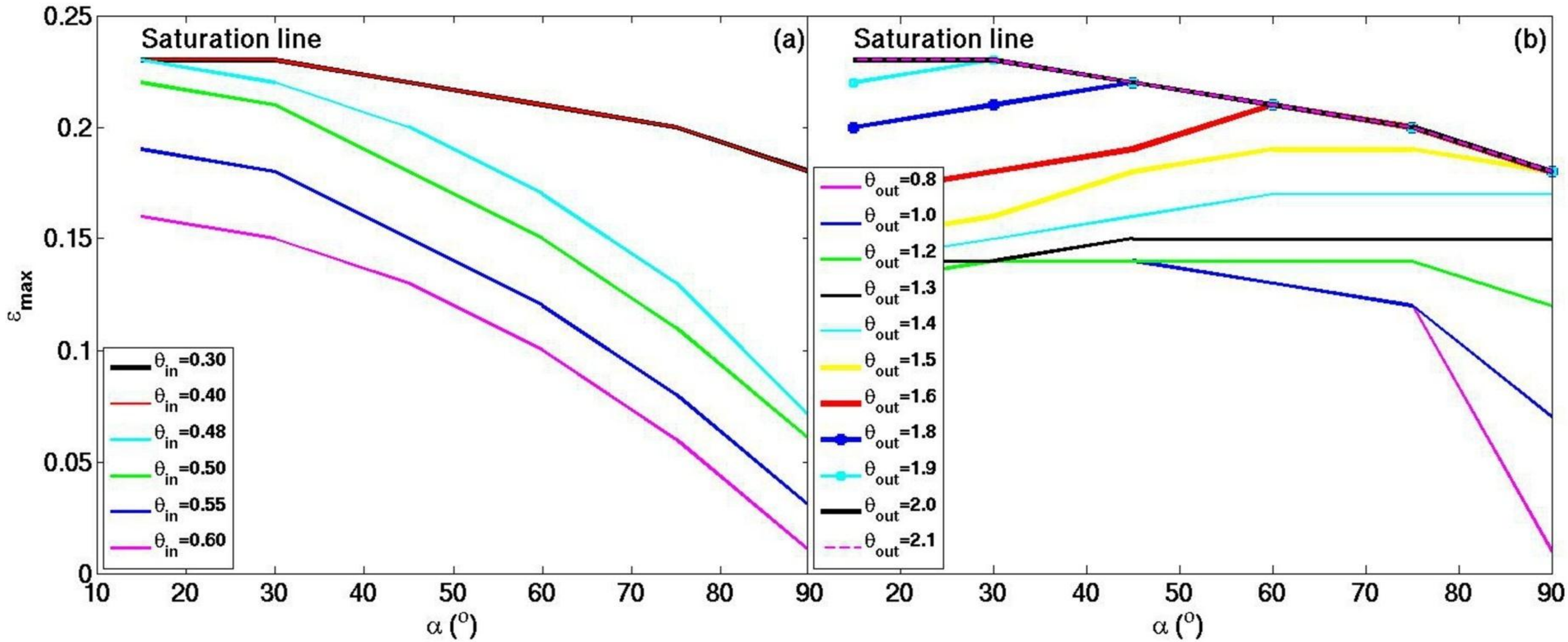

E-field of the SG offset-dipole

- High-altitude *E*-field (static-dipole + SG case (x x^a) (Muslimov &Harding 04)

$$E_{\parallel,\mathrm{high}} \approx -\frac{3}{8}\left(\frac{\Omega R}{c}\right)^3 \frac{B_0}{f(1)}\nu_{\mathrm{SG}} x^a \left\{\left[1+\frac{1}{3}\kappa\left(5-\frac{8}{\eta_c^3}\right)+2\frac{\eta}{\eta_{\mathrm{LC}}}\right]\times\cos\alpha+\frac{3}{2}\theta_0 H(1)\sin\alpha\cos\phi'\right\}(1-\xi_*^2)$$

- Low-altitude *E*-field (offset-dipole + SG case):

$$E_{\parallel,\mathrm{low}} \approx -3\mathcal{E}_0\nu_{\mathrm{SG}}x^a\left\{\frac{\kappa}{\eta^4}e_{1\mathrm{A}}\cos\alpha+\frac{1}{4}\frac{\theta_0^{1+a}}{\eta}\times\left[e_{2\mathrm{A}}\cos\phi'+\frac{1}{4}\epsilon\kappa e_{3\mathrm{A}}(2\cos\phi_0-\cos(2\phi'-\phi_0))\right]\sin\alpha\right\}(1-\xi_*^2)$$

- Total *E*-field for SG:

$$E_{\parallel,\mathrm{SG}} \simeq E_{\parallel,\mathrm{low}}\exp\left(\frac{-(\eta-1)}{(\eta_c-1)}\right)+E_{\parallel,\mathrm{high}}$$

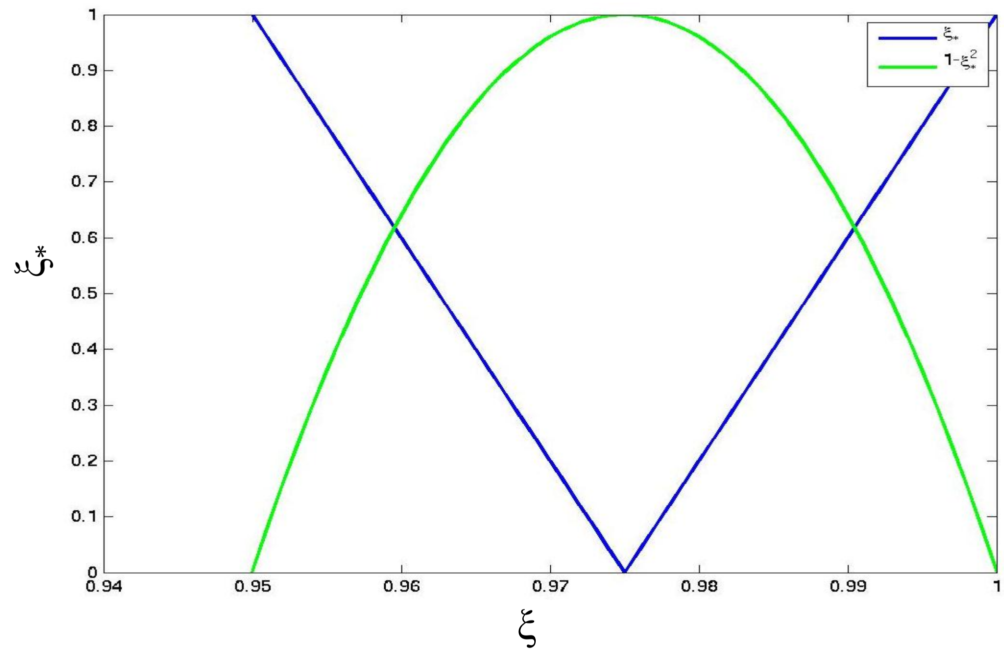

- Need the *E*-field to solve γ and the CR loss rate to correct the emissivity.

Particle transport equation

RR limit: $\boxed{\dot{\gamma} = 0}$

$\eta_c = 1.4\,;\ \phi' = 1.60\,;\ \xi_* = 0$

$$\dot{\gamma} = \dot{\gamma}_{\rm gain} + \dot{\gamma}_{\rm loss} = \frac{eE_{||}}{mc} - \frac{2e^2\gamma^4}{3\rho_{\rm curv}^2 mc}$$

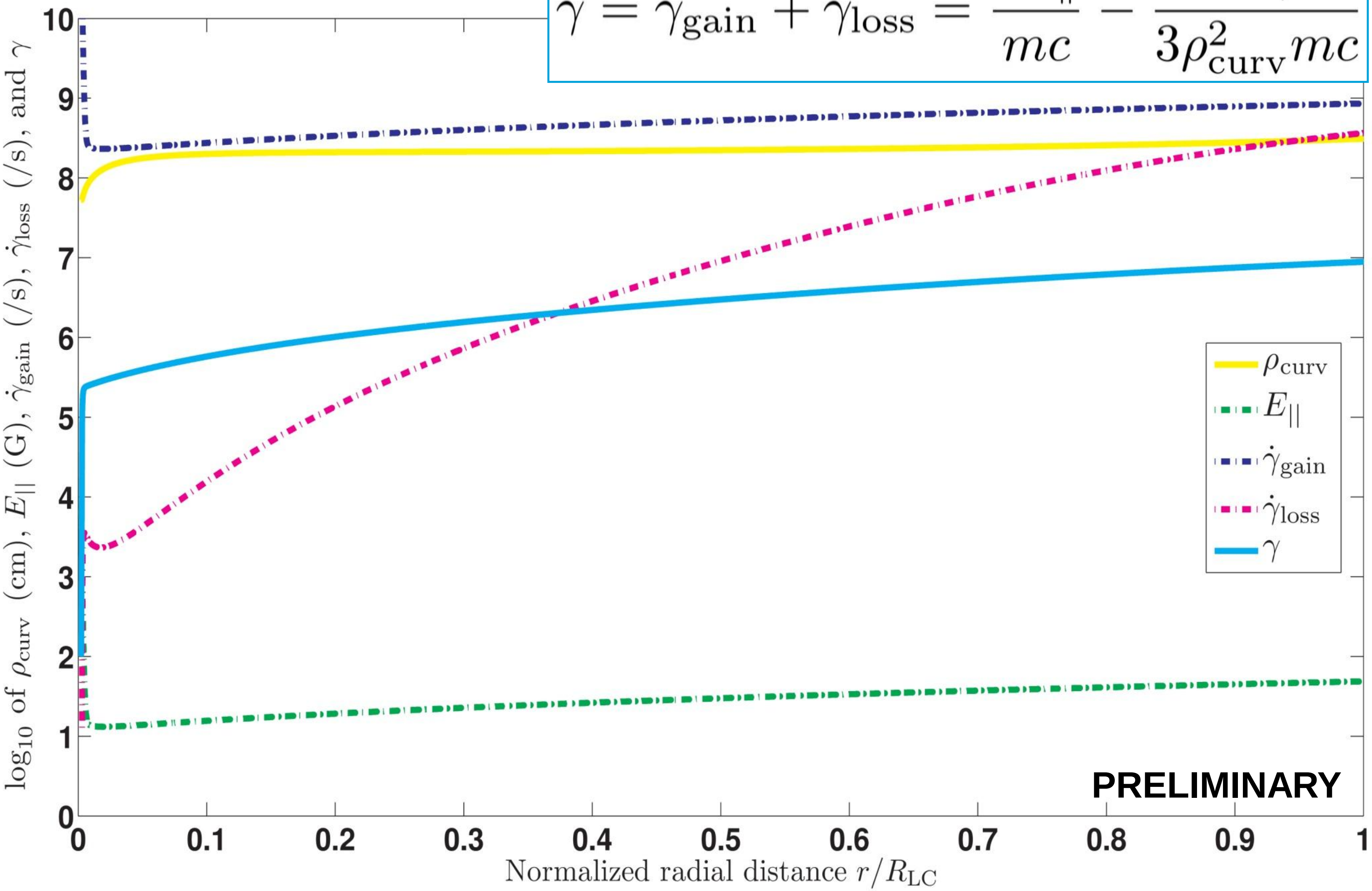

Phaseplots and LCs: Comparison of the static-dipole and offset-dipole fields

Used $(\alpha, \zeta, \epsilon) = (60^\circ, 85^\circ, 0.2)$. **(Representative solutions)**

Top panels: Constant emissivity for static-dipole

Bottom panels: Constant emissivity for offset-dipole

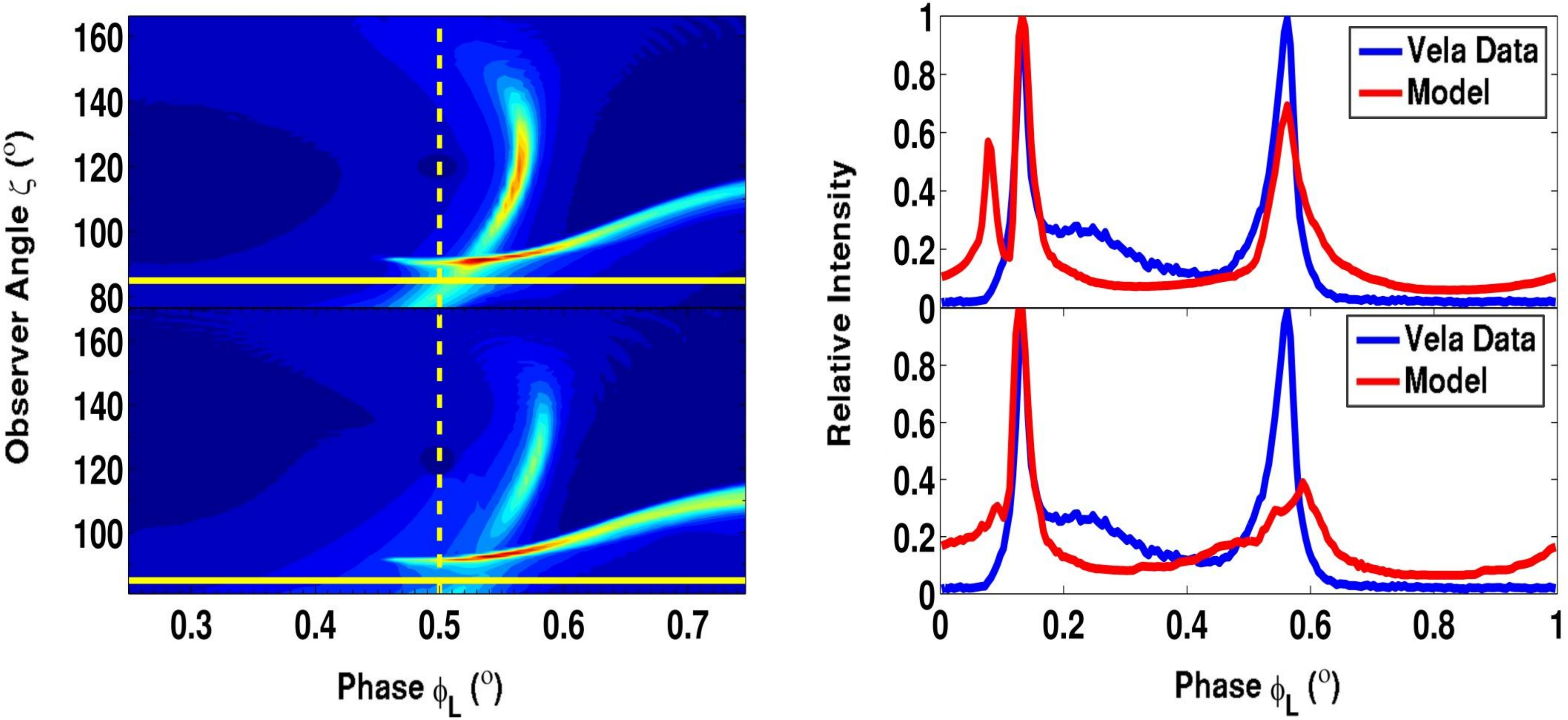

Phaseplots and LCs for the offset-dipole *B*-field

Used (α, ζ, ϵ) = (60°, 85°,0.2). **(Representative solutions)**

Top panels: Constant emisivity

Bottom panels: Solved for γ

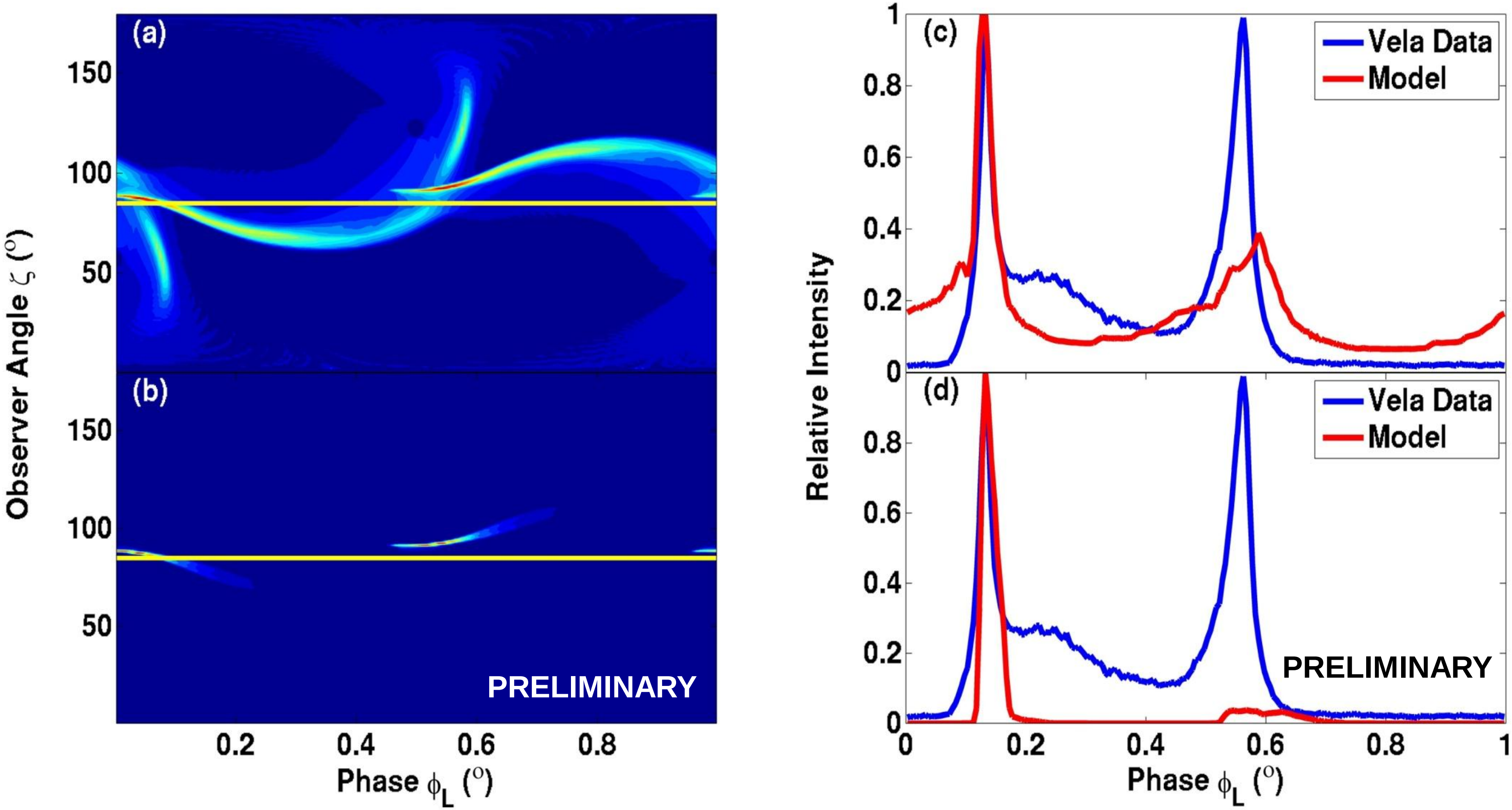

Conclusions

- We observed an **offset PC** in comparison with the static dipole *B*-field (assuming constant emissivity).

- The phaseplot is **qualitatively different** when we include an *E*-field and solve γ, given the fact that γ only becomes large enough to yield significant curvature radiation at large altitudes.

- Particles DO NOT attain the **radiation-reaction limit**, due to the low *E*-field.

Future work

- Extend the range of the **offset parameter** ϵ for which we are able to solve the PC rim.

- **Solve** η_c on each field line, instead of using a constant value where we match the E-field solutions.

- Need to **improve** our handling of the field lines where $E_{\|}$ changes sign with altitude.

- Lastly, search for **best-fit LCs**, thereby constraining Vela's magnetic field and emission geometry (α, ζ, ϵ).

Acknowledgements

This work is supported by the South African National Research Foundation (NRF).

A.K.H. acknowledges the support from the NASA Astrophysics Theory Program.

CV, TJJ, and AKH acknowledge support from the *Fermi* Guest Investigator Program.

“God’s love and kindness will shine
upon us like the sun that rises in the sky.”
Luke 1:73